

REPORTS

are insensitive to v . With $N_e = 1.3 \times 10^7$ (12) and with v ranging from 10^{-8} through 10^{-4} , predicted $\Delta W_{\text{diploid}}/\Delta W_{\text{haploid}}$ ranges from 1.11 to 1.05. We therefore expect haploids to adapt more rapidly unless $h > 0.95$ or $v < 10^{-8}$.

12. Materials and methods are available as supporting material on Science Online.
13. Paquin and Adams (10) estimated the numbers of adaptive mutations fixed in haploid and diploid populations by counting sudden changes in the frequencies of genetic markers hitchhiking with adaptive mutations. They concluded that fixations were 60% more frequent in diploids. Using competitions between genotypes sampled from their populations before and after inferred fixation events, they estimated the average selective advantage and dominance coefficient for adaptive mutations as $s = 0.1$ and $h = 0.9$. However, the times to fixation for such mutations would be much greater than the inferred times (8, 17). Computer simulations of Paquin and Adams' experiment (8) were incompatible with the inferred advantage for diploids.
14. M. Hiraoka, K. Watanabe, K. Umezu, H. Maki, *Genetics* **156**, 1531 (2000).
15. H. A. Orr, *Evolution* **52**, 935 (1998).
16. C. Zeyl, T. Vanderford, M. Carter, data not shown.
17. D. E. Dykhuizen, *Annu. Rev. Ecol. Syst.* **21**, 373 (1990).
18. Supported by NSF grant no. DEB-0075594 and a Young Investigator Award for Studies in Molecular Evolution from the Alfred P. Sloan Foundation (C.Z.)

and by Wake Forest University Research Fellowships (T.V.). We thank S. Otto and A. Grant for kindly performing flow cytometric analysis of DNA content in our evolved populations and S. Otto, B. Grimberg, and three anonymous reviewers for helpful comments that greatly improved the manuscript over previous versions. We also thank A. Pearce for her diligent and proficient technical assistance.

Supporting Online Material

www.sciencemag.org/cgi/content/full/299/5606/555/DC1

Materials and Methods
References and Notes

13 September 2002; accepted 20 November 2002

Tracheal Respiration in Insects Visualized with Synchrotron X-ray Imaging

Mark W. Westneat,^{*1} Oliver Betz,^{1,2} Richard W. Blob,^{1,3} Kamel Fezzaa,⁴ W. James Cooper,^{1,5} Wah-Keat Lee⁴

Insects are known to exchange respiratory gases in their system of tracheal tubes by using either diffusion or changes in internal pressure that are produced through body motion or hemolymph circulation. However, the inability to see inside living insects has limited our understanding of their respiration mechanisms. We used a synchrotron beam to obtain x-ray videos of living, breathing insects. Beetles, crickets, and ants exhibited rapid cycles of tracheal compression and expansion in the head and thorax. Body movements and hemolymph circulation cannot account for these cycles; therefore, our observations demonstrate a previously unknown mechanism of respiration in insects analogous to the inflation and deflation of vertebrate lungs.

Respiratory mechanisms in insects are important to our understanding of the physiology, behavior, and evolution of this diverse animal group. Most insects respire through a system of tubes called tracheae that connect to the air via spiracles that can be actively opened or closed (1). Tracheal tubes form a complex network of gas-filled vessels that divide throughout the body segments, legs, and wings. The tiniest tubes, called tracheoles, may be 1 μm in diameter, and they function to exchange gas with tissues of the body. Mechanisms for insect respiration include passive gas diffusion (2, 3), changes in internal pressure due to hemolymph pumping by the heart or by muscle contraction in the abdomen (4, 5), and autoventilation, during which body movements change the volume of tracheal tubes or air sacs associated with the tracheae (6–8). Despite recent insights into these

active mechanisms for changing the volume of the tracheal system (8, 9), the internal mechanics of insect respiration are largely unknown.

To directly observe changes in volume of the insect tracheal system, we obtained high-resolution x-ray videos of living insects using 15- to 25-keV synchrotron x-rays [supporting online material (SOM) Text]. The high flux and partial coherence of the x-ray source allow for real-time, phase-enhanced imaging (10) in which edge enhancement of the images enables clear visualization of insect anatomy. X-ray videos were recorded for the anterior thorax and head regions of ground beetles (*Platynus decentis*), carpenter ants (*Camponotus pennsylvanicus*), house crickets (*Achaeta domestica*), and other insects in either dorsal or lateral view.

The tracheal system at rest was inflated and was clearly visible as bright branching patterns on the x-ray video (Fig. 1; Movie S1). During compression, tracheae were squeezed to a progressively smaller diameter tube over the course of 300 to 500 ms and then were expanded over a similar time course. No changes in length of tracheae were observed. Tracheae were compressed in one primary direction (either laterally or dorsoventrally) so that the roughly circular cross section of the trachea at rest was compressed into an el-

lipse. For example, in beetles, lateral compression of the main thoracic tracheae was indicated by a decrease in tracheal width when viewed dorsally, and this appeared as a slight increase in width from a lateral view (Fig. 1). Narrowing of the tracheae was often synchronous throughout the head and thorax, but local tracheal compression was also observed.

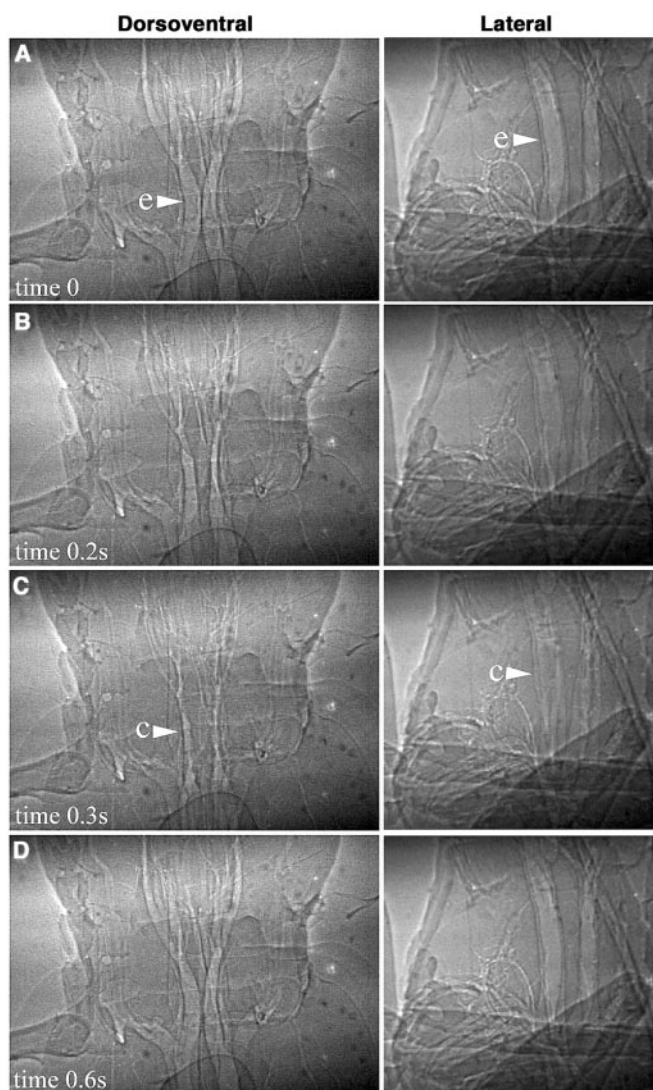
Respiratory frequency (Fig. 2) ranged from about 0.4 Hz to 0.7 Hz in the beetle (SOM Text). Duration of compression ranged from about 0.7 to 1.6 s in the three species (Fig. 2), followed by a period of inactivity. These data indicate interspecific variability in both exhalation-inhalation duration and cycle frequency. Volume change of tracheal tubes during respiration was calculated with the use of data on length and width of the tracheae during respiratory cycles (SOM Text). Volume change in the major tracheae of the anterior thorax and basal head of all three species was nearly 50% (Fig. 3). Mean resting volume of the main tracheal trunks of beetles was 0.065 mm^3 , and at maximal compression there was a volume decrease of 0.03 mm^3 , representing a tidal volume of 46%. Ants had the same average respiratory capacity (tidal volume of 46%), whereas crickets expelled less gas, with a tidal volume of 36%. All three species also showed deflation of the small subdivisions of the tracheae, suggesting that similar volume changes may be achieved throughout the tracheal system.

The rapid tracheal compression in insects signifies a previously undescribed active mechanism of respiration. We observed other respiratory mechanisms, such as abdominal pumping (4, 9), autoventilation (6), and circulatory fluid motion. However, these mechanisms cannot account for the rapid changes in head and thorax volume shown by synchrotron imaging. Tracheal compression in insects functions as a mechanism of air convection much like that of vertebrate lungs. The resting lung ventilation of a human, for example, is about 10% but may reach 75% during exercise; similar values have been measured for birds (6, 12). The insects studied here with 50% tidal volume were likely respiring at high rates, perhaps similar to the

¹Department of Zoology, Field Museum of Natural History, Chicago, IL 60605, USA. ²Department of Zoology, University of Kiel, Germany. ³Department of Biological Sciences, Clemson University, Clemson, SC 29634, USA. ⁴Experimental Facilities Division, Advanced Photon Source, Argonne National Laboratory, Argonne, IL 60439, USA. ⁵Department of Organismal Biology and Anatomy, University of Chicago, Chicago, IL 60637, USA.

*To whom correspondence should be addressed. E-mail: mwestneat@fieldmuseum.org

Fig. 1. Respiration by tracheal compression in the head and thorax of the beetle *Platynus decentis* (see Movie S1). Left panels are dorsoventral view (head, up; sides, left and right), right panels are lateral view (head, up; ventral, left) of different beetles. Tracheal tubes are expanded at rest [(A), arrowhead e], and compression (B) occurs throughout the anterior region of the insect. Lateral compression results in narrower tracheae in dorsal view and wider tracheae in lateral view. Maximal compression [(C), arrowhead c] is followed quickly by expansion of the tracheae (D). The entire respiratory cycle is completed in less than 1 s.



rates used during exercise, stress, or flight (3, 13). A second function of tracheal compression is to aid oxygen diffusion to tissues. If tracheal compression occurs with the spiracles closed, increased pressure will raise the diffusion gradient of oxygen across the tracheole-tissue boundary.

The mechanism of tracheal compression is likely driven by contraction of jaw muscles or limb muscles, causing elevated pressure inside the exoskeleton (14–17). Upon relaxation of the muscle, the tracheae expand due to the support from rings of taenidia in the tracheal wall (1) in a manner similar to recoil aspiration in air-breathing fishes (18). This mechanism implies the linking of locomotor muscles to respiration, which has been found to be widespread among animals (19).

Active tracheal breathing in the head and thorax may have played an important role in the evolution of terrestrial locomotion, running performance, and flight in insects, and it may be a prerequisite for oxygen delivery to complex sensory systems and ac-

tive feeding mechanisms. Tracheal compression appears widespread but not ubiquitous among insect lineages. We observed this mechanism of active tracheal respiration in some members of diverse groups of endopterygote insects (beetles, butterflies, flies) as well as in Hemiptera (bugs), the Orthoptera (cricket), Dermaptera (earwigs), Blattodea (cockroaches), and more basal insect lineages such as Odonata (dragonflies). The spectacular diversity of insects likely includes a range of respiratory mechanisms, some of which depend on the compression and expansion of the tracheal system in a lung-like manner as the means to exchange gases with the environment.

References and Notes

1. R. F. Chapman, *The Insects: Structure and Function* (Cambridge Univ. Press, Cambridge, UK, ed. 4, 1998).
2. A. Krogh, *Pflügers Arch. Gesamte Physiol. Menschen Tiere* **179**, 95 (1920).
3. P. J. Mill, in *Comprehensive Insect Physiology, Biochemistry, and Pharmacology*, G. A. Kerkut, L. I. Gilbert, Eds. (Pergamon, Oxford, UK, 1985), pp. 517–593.
4. P. L. Miller, in *Locomotion and Energetics in Arthro-*

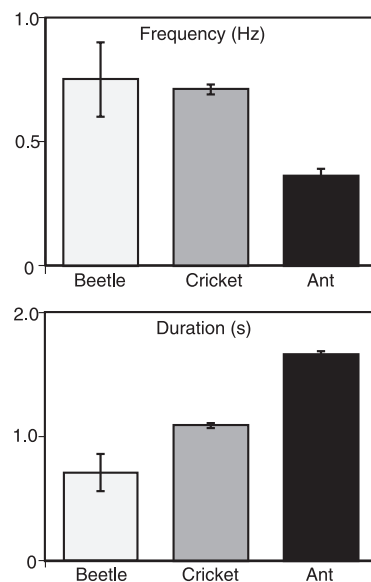


Fig. 2. Cycle frequency and compression duration of respiration in three insect species: the wood beetle, house cricket, and carpenter ant. Frequency of respiratory cycles was variable, ranging from 0.4 to 0.7 Hz, and the total time of tracheal compression ranged from about 0.7 to 1.6 s among species. Error bars, 1 standard deviation.

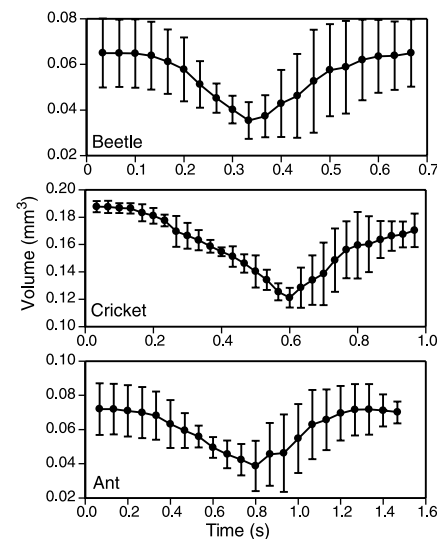


Fig. 3. Volume change in the main tracheae of the anterior thorax and head of the wood beetle, house cricket, and carpenter ant during respiratory cycles. Error bars, standard deviation of the mean of three respiratory pumping events in different individuals.

ods, C. F. Herreid, C. R. Fournier, Eds. (Plenum, New York, 1981), pp. 367–390.

5. L. T. Wasserthal, *Adv. Insect Physiol.* **26**, 297 (1996).
6. T. Weis-Fogh, *J. Exp. Biol.* **41**, 207 (1964).
7. K. Sláma, *Biol. Bull.* **175**, 289 (1988).
8. ———, *Ann. Entomol. Soc. Am.* **92**, 906 (1999).
9. U. Tartes, A. Kuusik, K. Hiiesaar, L. Metspalu, A. Vanatoa, *Physiol. Entomol.* **25**, 151 (2000).
10. P. Cloetens, R. Barrett, J. Baruchel, J. Guigay, M. Schlenker, *J. Phys. D* **29**, 133 (1996).
11. Materials and Methods are available as supporting material on Science Online.

REPORTS

12. K. Schmidt-Nielsen, *Animal Physiology* (Cambridge Univ. Press, Cambridge, UK, ed. 2, 1979).
13. Y. Komai, *J. Exp. Biol.* **201**, 2359 (1998).
14. A. V. Hill, *J. Physiol.* **107**, 518 (1948).
15. S. A. Wainwright, F. Vosburgh, J. H. Hebrank, *Science* **202**, 747 (1978).
16. M. W. Westneat, M. E. Hale, M. J. McHenry, J. H. Long Jr., *J. Exp. Biol.* **201**, 3041 (1998).
17. W. M. Kier, K. K. Smith, *Zool. J. Linn. Soc.* **83**, 307 (1985).
18. E. L. Brainerd, K. F. Liem, C. T. Samper, *Science* **246**, 1593 (1989).
19. D. R. Carrier, *J. Exp. Biol.* **199**, 1455 (1996).
20. Supported by DOE Office of Science, contract no. W-31-109-Eng-38, and by grants ONR N000149910184 and NSF DEB-9815614.

Supporting Online Material
www.sciencemag.org/cgi/content/full/299/5606/558/DC1
 Materials and Methods
 Movie S1

3 September 2002; accepted 6 December 2002

Chromatin Loosening by Poly(ADP)-Ribose Polymerase (PARP) at *Drosophila* Puff Loci

Alexei Tulin and Allan Spradling

Steroid response and stress-activated genes such as *hsp70* undergo puffing in *Drosophila* larval salivary glands, a local loosening of polytene chromatin structure associated with gene induction. We find that puffs acquire elevated levels of adenosine diphosphate (ADP)-ribose modified proteins and that poly(ADP)-ribose polymerase (PARP) is required to produce normal-sized puffs and normal amounts of Hsp70 after heat exposure. We propose that chromosomal PARP molecules become activated by developmental or environmental cues and strip nearby chromatin proteins off DNA to generate a puff. Such local loosening may facilitate transcription and may transiently make protein complexes more accessible to modification, promoting chromatin remodeling during development.

Cells within developing multicellular eukaryotes build complex tissue-specific chromatin architectures to express certain genes and silence others

Howard Hughes Medical Research Laboratories, Embryology Department, Carnegie Institution of Washington, 115 West University Parkway, Baltimore, MD 21210, USA.

(1). The enzyme PARP is thought to play a critically important role in preserving differentiated chromatin during DNA repair (2). The protein's zinc fingers specifically recognize DNA damage, and PARP activity increases strongly upon binding to such sites. The activated enzyme modifies nearby chromatin proteins with ADP-ribose moieties, disrupting their macromolecular complexes,

and causing the affected chromatin to decondense. The newly repaired region returns to a normal state after PARP down-regulates its own activity via automodification, and the chromatin proteins, freed of ADP-ribose groups by a specific glycohydrolase, reassemble. Recent genetic studies with *Drosophila melanogaster* show that PARP is an essential gene required to organize chromatin throughout the life cycle (3). However, the relation between PARP action during repair and during development remains unclear.

Drosophila chromatin normally undergoes many programmed changes that could be mediated by PARP (1). In particular, chromatin alterations manifest as salivary gland polytene chromosome puffs occur at the sites of ecdysone response genes before molting (4). To look for specific loci where PARP may act, we surveyed the levels of PARP protein, ADP-ribosylation activity, and ADP-ribose polymers during embryonic and larval development. Epitope-tagged PARP protein is widely distributed throughout the euchromatin of both diploid and polytene *Drosophila* nuclei (Fig. 1, A and B). However, the activity state of these PARP molecules varies widely because injected biotinylated nicotinamide adenine dinucleotide (NAD), the source of ADP-ribose adducts, differentially labels only a limited number of polytene chromosome regions,

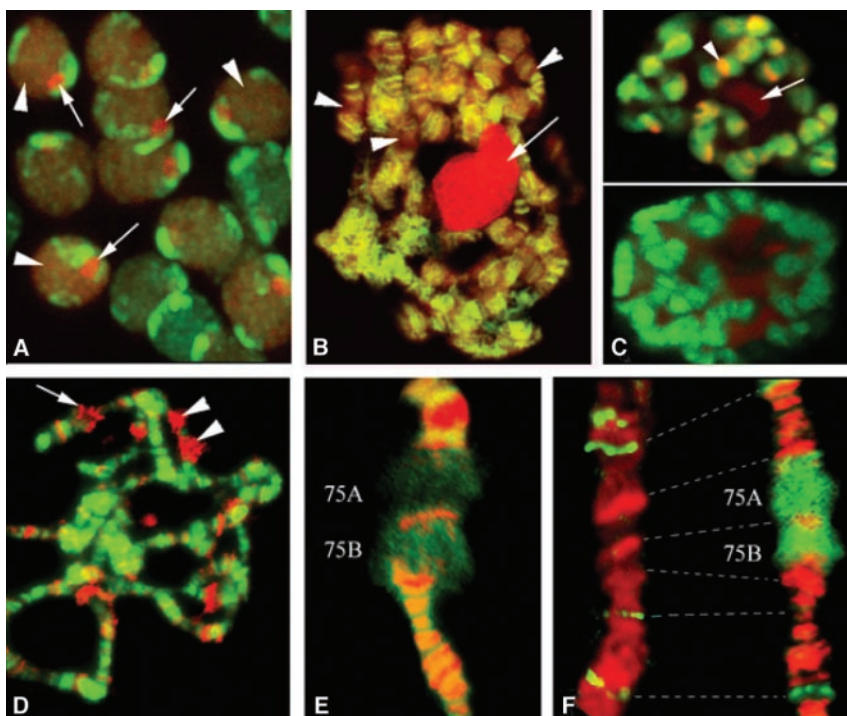


Fig. 1. Differential accumulation of poly(ADP-ribose) in polytene chromosome puffs. DNA shows as green in (A) through (D), red in (E) and (F). PARP-DsRed (red) (3) is widespread in the euchromatin (arrowheads) of (A) larval diploid brain cells (B) and polytene salivary gland cells as well as in nucleoli (arrows). (C) PARP activity, indicated by incorporation of biotinylated-NAD (red) 1 hour after larval injection, is high at certain sites (arrowhead) and in the nucleolus (arrow). Incorporation is due to PARP because it is abolished by injection of 3-AB (lower panel) 30 min before assay. (D) Poly(ADP-ribose) polymer (red) is enriched at specific polytene chromosomes sites, including puffs. Note early ecdysone-induced puffs at 2B (arrow) and 75A and 75B (arrowheads). (E) PARP-GFP (3) is present throughout this chromosome region (green). (F) However, poly(ADP-ribose) (green) is not found at 75A or 75B before puffing (left) but is found after puffing (right) (fig. S1).